C

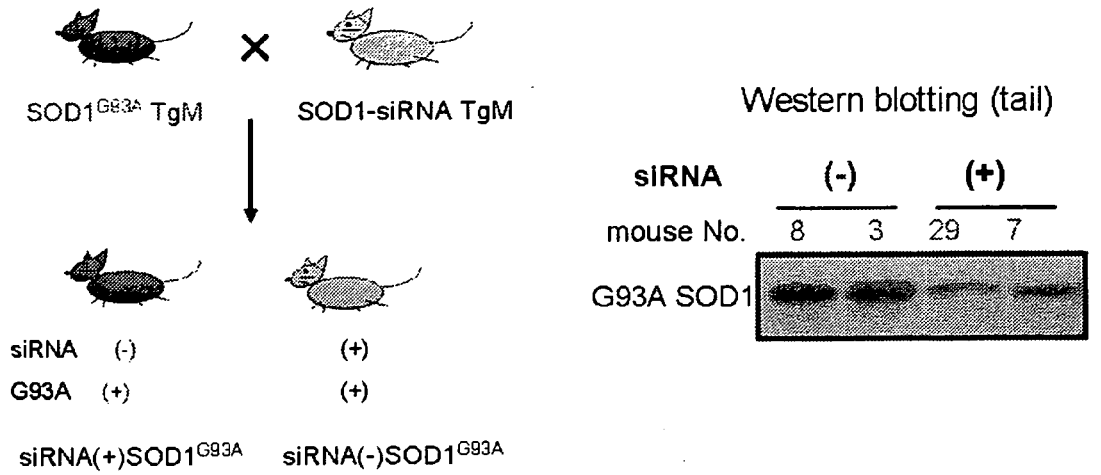

D

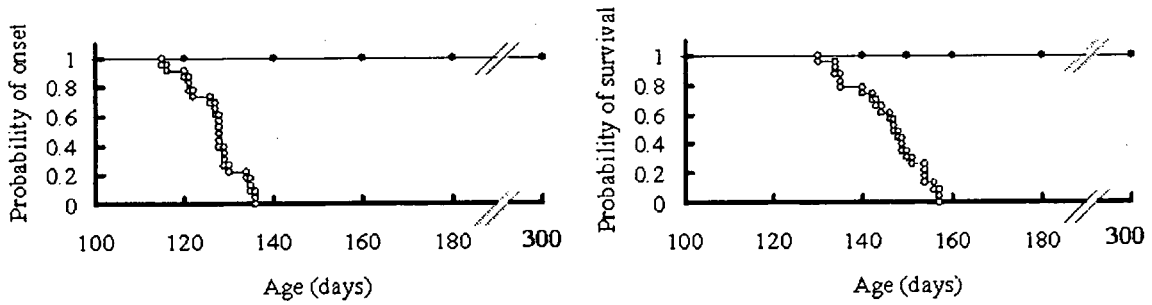

Figure 1C, D. Double Tg mice had a marked reduction in the amount of G93A SOD1 protein in the spinal cord and did not show the ALS phenotype. C, Levels of both mutant G93A SOD1 and mouse SOD1 proteins were similarly reduced in the spinal cords of double Tg mice on Western blot analysis. The level of G93A SOD1 protein in double Tg mice was lower than that the low copy strain of *SOD1*^{G93A} Tg mice. *Lane 1: SOD1*^{G93A} Tg mouse, *Lane 2*: low copy strain of *SOD1*^{G93A} Tg mouse, *Lane 3*: double Tg mouse and *Lane 4*: wild-type mouse. D, This *SOD1*^{G93A} Tg mouse at 130 days of age showed paralysis of both hindlimbs. In contrast, the double Tg mouse at the same age walked well. D, Cumulative probabilities of onset of disease signs (*Left*) and survival (*Right*). There was a significant increase in the lifespan of the double Tg mice (n=6; closed circles) compared with the *SOD1*^{G93A} Tg mice (n=23; open circles).

Optimal location of mutation for discriminating point mutation in familial ALS

In order to search the best position for discriminating point mutation, we examined suppression effect of several siRNAs to G93A SOD1, the mutation of familial ALS on expression of wild type SOD1. For monitoring SOD1 expression, coding sequence of wild type SOD1 cDNA was subcloned into 5' side of luciferese gene.

When mismatch position was changed between 5^{th} to 16^{th} from the 5' end, mismatch in siRNA at 13^{th} position showed most marked decrease of cleavage siRNA activity to the mismatch mRNA.

Diversing effects of mismatch between siRNA and target sequences have been reported. The central single mutation, mismatch in siRNA at 10^{th} and 11^{th} position, produces marked decrease of cleavage siRNA activity. The mismatch in the 5'end has negligible effect on siRNA cleavage activity compared with more centrally located mutation. This bias might be linked to the proposed existence of a 'ruler' region in the siRNA which is used by the RISC complex to 'measure' the target RNA for cleavage. In six siRNAs examined in our study, siRNAs with 10th and 13th mismatch from 5' end of sense sequence have better discrimination than that with outside mismatch. Especially, 5' side mismatch does not affect much the siRNA cleavage activity. Our result is consistent with the previously reported results.

siRNA specific for G93A SOD1 with point mutation in familial amyotrophic lateral sclerosis (ALS) (2)

The familial ALS is caused by point mutation in SOD1 gene. We try to make siRNA which cleave the mutant SOD1 with G93A point mutation, leaving wild-type intact.

Two siRNAs targeting G93A SOD1 corresponding to regions 277–297 (siRNA G93A.1) and 275-294 (siRNA G93A.2) were designed. Western blot analysis revealed that both siRNA G93A.2 reduced the expression of G93A SOD1 protein by about 90% when expression efficiency was adjusted with co-transfected GFP (Fig. 2A). The suppression of G93A SOD1 protein by siRNA G93A. 2 increased in a dose-dependent manner when the amount of siRNA was changed from 2.5 to 125 nM(data not shown). The siRNA recognized only one nucleotide alteration, because they suppressed wild-type SOD1 protein much less than G93A SOD1-especially siRNAG93A.2, for which the reduction of wild type was only 1.8% (Fig.2A). The suppression effect was confirmed by the reduction in GFP fluorescence when siRNA was co-transfected with a GFP-fused SOD1 plasmid (Fig. 2B).

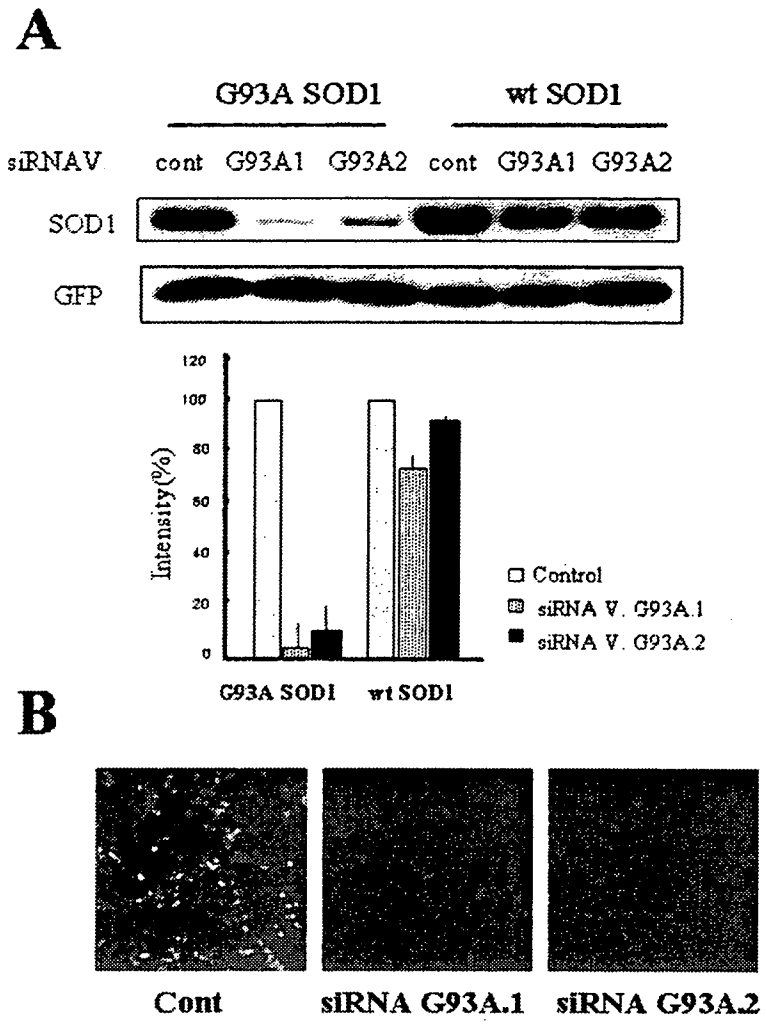

Figure 2. Effect of DNA-vector based expressing siRNAs (siRNA V.) (A) Effect of of expressing siRNA vectors for G93A SOD1, siRNA V. G93A 1 and 2, on G93A and wild-type SOD1 protein expressed on Western blotting. siRNA V. G93A 1 and 2 selectively suppressed the expression of mutant SOD1. Data are at 48 hours after transfections. Values in the figure are the mean and SEM. (B) Effect of siRNA V. G93A 1 and 2, on G93A and wild-type SOD1 protein expressed on GFP fluorescence expressed by co-transfected SOD1-GFP expressing vectors in Neuro2a cells. Expression level of target protein was adjusted by level of co-transfected DsRed expression.

siRNA specific for mutant allele in Machado-Joseph disease (MJD) using polymorphorism related to CAG repeat length (8)

Machado-Joseph disease (MJD) is an autosomal dominant neurodegenerative disorder which is characterized clinically by cerebellar ataxia, pyramidal and extrapyramidal signs, peripheral neuropathy and ophthal moplegia. The number of CAG in MJD1 gene repeats is between 13 and 36, whereas in patients this range is expanded from 62 to 84. The pathogenosis of MJD is considered to be due to 'gain of toxic function' of mutant MJD protein.

Therefore, a most effective and simple gene therapeutic approach for MJD requires the reduction of the aberrant mutant protein. Furthermore, it might be needed to reduce mutant ataxin-3 selectively, leaving wild-type protein intact, because wild type MJD1 gene product, ataxin-3, should have an important role in cell survival, such as quality control of endoplasmic reticulum, and DNA repair. We found that CAG repeat tract in MJD1 gene is followed by C or G and there is extreme bias of this C/G polymorphism between mutant and normal MJD1 alleles; mutant alleles have exclusively the (CAG)nC, whereas normal alleles have both (CAG)nG and (CAG)nC in a similar frequency (Fig. 3A). Here, we engineered siRNAs to cleave selectively mutant MJD RNA targeting the sequence including this C/G polymorphism.

The mutant ataxin-3, Q79C, was most effectively suppressed by 25 nM MJD siRNA MJD3, and was decreased by 96.0% on signal intensity of Western blotting compared with that in control (Fig 3B). In contrast, the expression of the wild type ataxin-3, Q22G, was moderately suppressed by the siRNA.

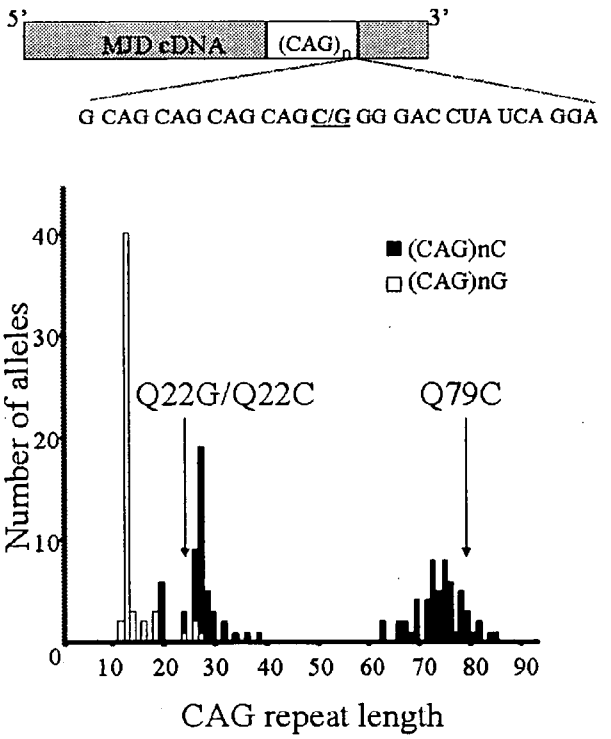

Figure 3A. Design of small interfering RNA (siRNA) Sequences targeting the C/G Polymorphism in MJD1 gene. Schema of human MJD1 gene showing C/G Polymorphism just downstream of CAG repeat (upper panel). The Distribution of C/G Polymorphism and the CAG Repeat Length in 56 Japanese MJD Patients (lower panel). All expanded alleles have (CAG)nC, whereas the normal alleles have (CAG)nC and (CAG)nG in similar frequencies (0.46 and 0.54). Arrows indicate the CAG repeat numbers of ataxin 3-expression vector constructs used in this study as wild type and mutant.

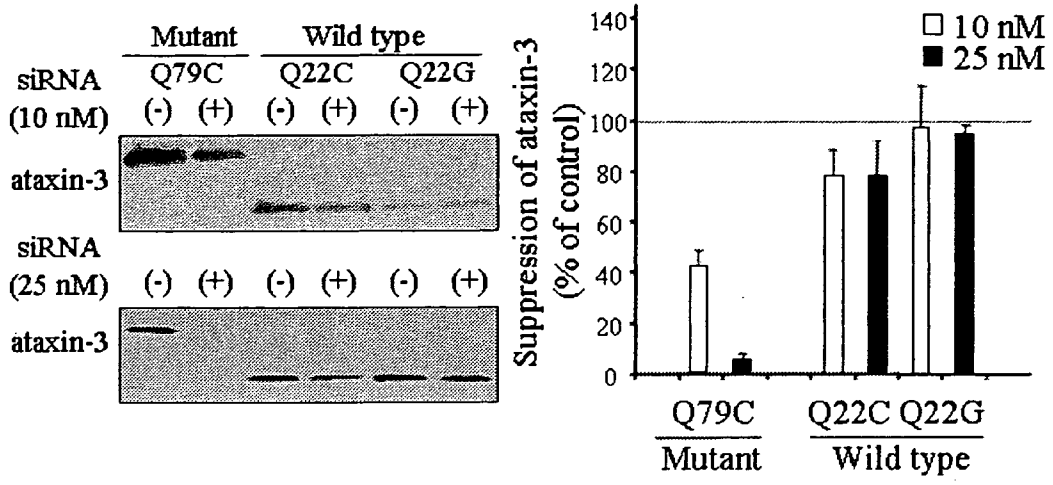

Figure 3B. Specific effect of the siRNA on the expression of mutant MJD1. Comparison of the Effect of siRNA MJD3 on Q79C, Q22G, and Q22C expression Western blot analysis of the effect of siRNA MJD3 at 10 nM and 25 nM on Q79C, Q22G, and Q22C expression. The results of siRNA(-) were made with siRNA MJD3-shuffle. Right upper panel indicates quantitation of signal intensities. Each percentage suppression was determined by the band intensity of the control. Values are the mean and SEM. Almost no suppression on Q22G expression (5.9%), and mild suppression on Q22C expression (22.5%) were noted by siRNAMJD3 at 25 nM siRNA in contrast to robust suppression on Q79C expression (96.0%).

Sequence-independent discriminations of mutant and wild-type alleles by siRNA

Unexpectedly, MJD siRNA did not decrease much (22.5%) the expression of another wild type allele, Q22C, although the target sequence in (CAG)79C and (CAG)22C were same (Fig 3B).

This is the first report of sequence-independent discrimination of mutant and wild-type alleles by siRNA. One possible reason for this difference is that not all RNA sequences are equally accessible to siRNAs: some sequences might be buried within the secondary structure of target RNAs especially when they are highly folded. We also experienced that the best target site of siRNA for the highly folded RNA was almost same as that for ribozyme, which cleavage efficiency is much influenced by the secondary structure of target RNA. The target site of C/G polymorphism is just downstream of the CAG repeat which represents a tight stem-form in their secondary structure on a computer prediction. Although we have no data indicating siRNA MJD3 is more accessible to (CAG)79C than (CAG)22C, a change of secondary structure of the MJD RNA due to a large difference of the CAG repeat length might affect the efficiency of siRNA MJD3. Another possible explanation is that there is a RNA-binding protein preferentially binding (CAG)22C than (CAG)79C which interferes the access of siRNA MJD3 to (CAG)22C RNA.

As demonstrated above, design of siRNA specific for the mutant allele of autosomal dominant disease is possible by even single nucleotide alternation and change in the secondary structure of the mRNA. Effect of transgenic siRNA to prevent autosomal dominant inherited neurological disease has been demonstrated in transgenic model. When efficient and safe delivery of siRNA in vivo and long-term expression of siRNA are achieved, gene therapy for autosomal dominant diseases is not a fairy tale.

References

1. Cleveland, D. W. 1999, *Neuron* 24, 515
2. Yokota, T., Miyagishi, M., Hino, T., Matsumura, R., Andrea, T., Urushitani, M., Rao, R. V., Takahashi, R., Bredesen, D. E., Taira, K., and Mizusawa H. 2004, *Biochem. Biophys. Res. Com.* 314, 283
3 Xia, H., Mao, Q., Eliason, S. L., Harper, S. Q., Martins, I. H., Orr, H. T., Paulson, H. L., Yang, L., Kotin, R. M., and Davidson, B. L. 2004, *Nat. Med.* 10, 816
4. Raoul, C., Abbas-Terki, T., Bensadoun, J-C., Guillot, S., Haase, G., Szulc, J., Henderson, C. E., and Aebischer, P. (2005) *Nat. Med.* 11, 423
5. Ralph, G. S., Radcliffe, P. A., Day, D. M., Carthy, J. M., Leroux, M. A., Lee, D. C. P., Wong, L-F., Bilsland, L. G., Greensmith, L., Kingsman, S. M., Mitrophanous, K. A., Mazarakis, N. D., and Azzouz, M. 2005, *Nat. Med.* 11, 429
6. Miller, T. M., Kasper, B. K., Kops, G. J., Yamanaka, K., Christian, L. J., Gage, F. H., and Cleveland, D. W. (2005) *Ann. Neurol.* 57, 773
7. Saito Y, Yokota T, Mitani T, Ito K, Anzai M, Miyagishi M, Taira K, Misusawa H. 2005, J Biol Chem, 280, 42826
8. Li Y, Yokota T, Taira K, Mizusawa H. 2004, Ann Neurol 56, 124

Efficient *In Vivo* Delivery of siRNA to the Liver by Conjugation of α-Tocopherol

Kazutaka Nishina[1,2], Toshinori Unno[1], Yoshitaka Uno[1], Takayuki Kubodera[1,2], Tadashi Kanouchi[1], Hidehiro Mizusawa[1,2] and Takanori Yokota[1]

[1]*Department of Neurology and Neurological Science, Graduate School, Tokyo Medical and Dental University, Bunkyo-ku, Tokyo, Japan;* [2]*21st Century Center of Excellence Program on Brain Integration and Its Disorders, Tokyo Medical and Dental University, Yushima, Bunkyo-ku, Tokyo, Japan*

RNA interference is a powerful tool for target-specific knockdown of gene expression. However, efficient and safe *in vivo* delivery of short interfering RNA (siRNA) to the target organ, which is essential for therapeutic applications, has not been established. In this study we used α-tocopherol (vitamin E), which has its own physiological transport pathway to most of the organs, as a carrier molecule of siRNA *in vivo*. The α-tocopherol was covalently bound to the antisense strand of 27/29-mer siRNA at the 5′-end (Toc-siRNA). The 27/29-mer Toc-siRNA was designed to be cleaved by Dicer, producing a mature form of 21/21-mer siRNA after releasing α-tocopherol. The C6 hydroxyl group of α-tocopherol, associated with antioxidant activity, was abolished. Using this new vector, intravenous injection of 2 mg/kg of Toc-siRNA, targeting *apolipoprotein B* (*apoB*), achieved efficient reduction of endogenous *apoB* messenger RNA (mRNA) in the liver. The downregulation of *apoB* mRNA was confirmed by the accumulation of lipid droplets in the liver as a phenotype. Neither induction of interferons (IFNs) nor other overt side effects were revealed by biochemical and pathological analyses. These findings indicate that Toc-siRNA is effective and safe for RNA interference–mediated gene silencing *in vivo*.

Received 13 October 2007; accepted 7 January 2008; advance online publication 12 February 2008. doi:10.1038/mt.2008.14

INTRODUCTION

Short interfering RNAs (siRNAs) have potential for therapeutic application in a wide spectrum of disorders including cancer, infectious diseases, and inherited diseases. Effective *in vivo* delivery of siRNAs to the specific target cells is the most important challenge in respect of clinical applications. *In vivo* gene silencing with RNA interference has been reported using either viral vectors[1] or high-pressure, high-volume intravenous injection of synthetic siRNAs,[2,3] but these approaches have limitations in clinical practice because of their side effects. Accordingly, a variety of nonviral systems are being developed for delivery of siRNA to liver, tumors, and other tissues *in vivo*.

Recent work in the area of nonviral delivery of synthetic siRNAs has used cationic liposomes[4–6] or nanoparticles.[7] Among these approaches, the most efficient systemic administration was achieved using stable nucleic acid lipid particles.[4] However, a therapeutic dose (2.5 mg/kg) of these particles, when administered in cynomolgus monkeys, caused marked liver damage.[4] A key drawback of cationic liposomes and nanoparticles is that their physical lipophilic property promotes passive transfer of siRNA complexes to the liver, potentially causing toxicity. More recently, a new class of receptor-mediated siRNA vectors, consisting of a synthetic compound and a ligand, has been reported. These ligands are (i) *N*-acetylgalactosamine[8] or galactose[9] ligands that target asialoglycoprotein receptors on hepatocytes, (ii) apolipoprotein A-I ligands that target scavenger receptor class B type I on the hepatocytes,[10] and (iii) rabies virus glycoprotein ligands that target acetylcholine receptors on the neurons.[11] These receptor-mediated delivery systems could increase efficiency and specificity of target cells *in vivo*. However, the synthetic molecules of these vectors were found to exert an immunostimulatory effect.[8]

We hypothesized that the most effective *in vivo* carrier would be a molecule that is essential for target tissue cells but cannot be synthesized within the cells. Vitamins fit these requirements well, and the only vitamin that is not toxic even at high doses is vitamin E.[12] α-Tocopherol (vitamin E) is a fat-soluble natural molecule that has many physiological pathways from serum to liver. The majority of the absorbed vitamin E is transferred into lipoproteins including chylomicrons, low-density lipoprotein, and high-density lipoprotein, and these constitute an important source of plasma vitamin E for hepatic uptake (reviewed in ref. 13). In addition, the three α-tocopherol-associated proteins (SEC14L2, SEC14L3, and SEC14L4), and the albumin-related protein, afamin, are known to be vitamin E–binding proteins in the serum (reviewed in ref. 14). In this study, we have tried to utilize these physiological pathways of vitamin E transport to the liver as an *in vivo* delivery system for siRNA.

RESULTS

Design of α-tocopherol-bound siRNA

Asymmetric double-strand RNA having 2 nucleotides (nt) in 3′-overhang only in the antisense strand is good for predicting a

The first two authors contributed equally to this work.

Correspondence: *Takanori Yokota, Department of Neurology and Neurological Science, Graduate School, Tokyo Medical and Dental University, 1-5-45 Yushima, Bunkyo-ku, Tokyo 113-8519, Japan. E-mail: tak-yokota.nuro@tmd.ac.jp*

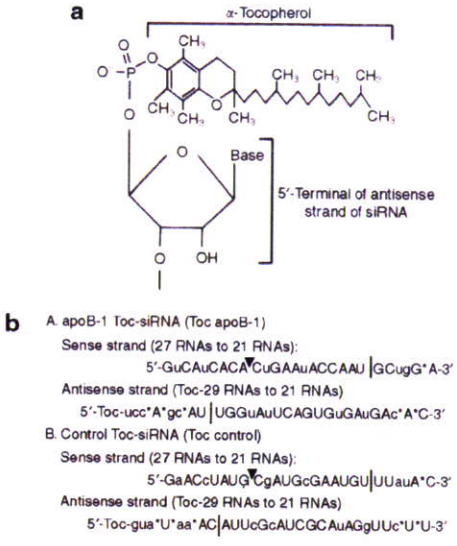

Figure 1 Design of α-tocopherol-bound short interfering RNA (siRNA). (**a**) Chemical structure of vitamin E (α-tocopherol)-bound siRNA. (**b**) Sequences and chemical modifications of α-tocopherol-bound siRNA for targeting *apoB* messenger RNA (apoB-1 Toc-siRNA) or for targeting unrelated gene (control Toc-siRNA). The lower-case letters represent sugar 2′-O-methylation, and asterisks represent phosphorothioate backbone linkage. The predicted cleavage sites by Dicer[15] and Argonaute2 (ref. 19) are indicated by black bars and arrowheads, respectively. The sequences in bold letters indicate the predicted 21-mer siRNA sequences after Dicer cleavage. Toc; α-tocopherol.

Dicer cleavage site and can therefore define the 21-mer siRNA sequence cleaved from 27/29-mer siRNA by Dicer.[15] The α-tocopherol was covalently bound to the 5′-end of the antisense strand of these siRNAs. The chemical structure of α-tocopherol-bound siRNA (Toc-siRNA) is shown in **Figure 1a**. The sequences of (i) Toc-siRNA for targeting mouse *apolipoprotein B* (*apoB*) messenger RNA (mRNA) (NM_009693) (apoB-1 Toc-siRNA)[16] and (ii) Toc-siRNA for targeting mouse *beta-site APP cleaving enzyme 1* (*BACE1*) mRNA (NM_011792) (control Toc-siRNA) are shown in **Figure 1b**.

For *in vivo* application of Toc-siRNA, it is essential to ensure the stability of siRNA against serum-derived nucleases. For this purpose, we made chemical modifications with phosphorothioate backbone linkage and sugar 2′-O-methylation on both the sense and the antisense strands. The portions of siRNA that were predicted to be cleaved out by Dicer, *i.e.*, 8 nt in the 5′-side of the antisense strand and 6 nt in the 3′-side of the sense strand, were substantially modified. Further, in order to increase stability against endonucleases while preserving siRNA activity,[17] partial internal modifications were made to the siRNA sequences with 2′-O-methylation, in addition to modifications at the termini.[18] The Dicer cleavage sites in both sense and antisense strands, and the Argonaute2 cleavage site[19] in the sense strand were spared any modification (**Figure 1b**).

Improved stability of siRNA with preserved cleaving efficiency by chemical modifications

The naked and the chemically modified siRNA in serum were compared for stability *in vitro*. With and without α-tocopherol,

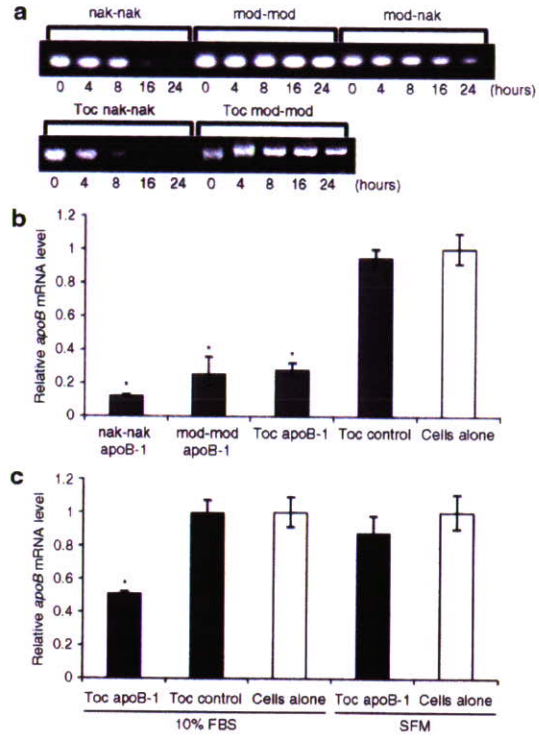

Figure 2 Improvement in stability and preservation of cleaving efficiency of short interfering RNA (siRNA) after chemical modification. (**a**) The stability of modified siRNA in the serum. The both-strands-naked siRNA (nak-nak), both-strands-modified siRNA (mod-mod), only-sense-strand-modified siRNA (mod-nak), both-strands-naked α-tocopherol-bound siRNA (Toc nak-nak), and both-strands-modified α-tocopherol-bound siRNA (Toc mod-mod) were incubated in the mouse serum at 37°C for 4, 8, 16, and 24 hours. The samples were treated with Proteinase K and electrophoresed in 2% agarose gel. (**b**) Reduction of *apoB* messenger RNA (mRNA) levels in the Hepa 1-6 cell line after transfection with apoB-1 siRNA using Lipofectamine RNAiMAX. The quantitative reverse transcriptase-polymerase chain reaction (qRT-PCR) analyses of *apoB* mRNA levels relative to *gapdh* mRNA were performed 24 hours after transfection of both-strand-naked apoB-1 siRNA (nak-nak apoB-1), both-strand-modified apoB-1 siRNA (mod-mod apoB-1), both-strand-modified apoB-1 Toc-siRNA (Toc apoB-1), and control Toc-siRNA (Toc control). The data shown are relative to the values in untreated cells (Cells alone). $n = 3$, Data are shown as mean values ± SEM. $^*P < 0.005$ as compared to cells-alone group. (**c**) Reduction of *apoB* mRNA levels in the Hepa 1-6 cell line after transfection using apoB-1 Toc-siRNA alone. The qRT-PCR analyses of *apoB* mRNA levels relative to *gapdh* mRNA were performed 24 hours after transfection with apoB-1 Toc-siRNA (Toc apoB-1) and control Toc-siRNA (Toc control). The Hepa 1-6 cells were maintained in Dulbecco's modified Eagle's medium (DMEM) only [serum-free medium (SFM)], or in DMEM supplemented with 10% fetal bovine serum (10% FBS). The data shown are relative to the values in untreated cells (Cells alone). $n = 3$, Data are shown as mean values ± SEM. $^*P < 0.005$ as compared to cells-alone group. Toc; α-tocopherol. *gapdh, glyceraldehyde-3-phosphate dehydrogenase.*

the stability of the siRNA with both strands modified was much greater than those of the siRNA with both strands naked, and the siRNA with only the sense strand modified. The conjugation of α-tocopherol did not increase the stability of siRNA (**Figure 2a**).

The impact of the silencing ability conferred by the chemical modification of siRNAs and binding of α-tocopherol was studied in cultured cells of mouse hepatocellular carcinoma (Hepa 1-6)

using a transfection reagent. Even with considerable chemical modification of both strands, the silencing effect of apoB-1 siRNA on endogenous *apoB* mRNA in the Hepa 1-6 cells was not much impaired when compared with the silencing effect of apoB-1 siRNA with both strands naked. Further, the binding of α-tocopherol to the apoB-1 siRNA with both strands modified also did not interfere with the silencing activity (**Figure 2b**). In effect, we succeeded in carrying out considerable appropriate chemical modifications in the siRNA sequences to increase serum stability, while preserving silencing activity.

Next, α-tocopherol-mediated induction of siRNA was confirmed in Hepa 1-6 cells without any transfection reagents. The addition of apoB-1 Toc-siRNA to the culture medium reduced endogenous *apoB* mRNA in Hepa 1-6 cells. This silencing effect disappeared when serum was absent in the cultured medium (**Figure 2c**). This finding suggests that α-tocopherol can introduce siRNA into the cells in association with molecules in the serum.

Effective delivery and processing of Toc-siRNA in mice liver

In order to investigate whether successful delivery of Toc-siRNA had been achieved, liver sections were taken from mice 1 hour after injection with Cy3-labeled Toc-siRNA (Cy3 bound to the sense strand of siRNA), and the sections were subjected to confocal imaging. We observed marked accumulation of Cy3 signal both in hepatocytes and nonparenchymal cells in the liver sinusoids. Almost all the hepatocytes had the Cy3 signal. There was predominant signal density around central veins. There was no Cy3 signal in the control liver sections from the mouse injected with Cy3-labeled siRNA without α-tocopherol (**Figure 3a**). We also confirmed a less prominent Cy3 signal in other organs including lung; the details of the systemic distribution of Toc-siRNA are to be published elsewhere.

In order to study whether Toc-siRNA is processed to a mature form of 21/21-mer siRNA, northern blotting was performed on mouse liver after injection of 32 mg/kg Toc-siRNA. The assay showed two bands of sizes ~21 nt and ~29 nt, corresponding to the processed 21-mer antisense strand and the 29-mer α-tocopherol-bound antisense strand, respectively (**Figure 3b**). These results clearly show that Toc-siRNA has the ability to enter mouse liver cells and be processed by Dicer in the cytosol.

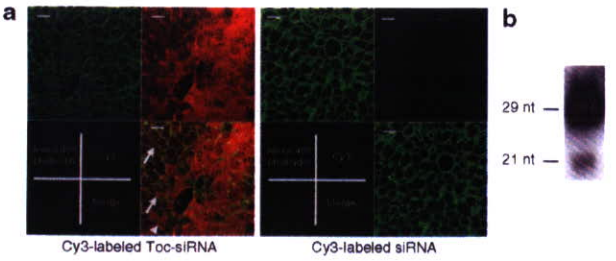

Figure 3 Targeted delivery of Toc siRNA to mice livers after injection. (**a**) Confocal images of liver sections from mice injected intravenously with Cy3-labeled Toc-siRNA (left panel) and Cy3-labeled siRNA (right panel). Cy3 signal (red) was noted in hepatocytes (arrowhead) and nonparenchymal cells (arrows). Liver sections were stained with Alexa-488 phalloidin to visualize cell outlines (green). Scale bar = 20 μm. (**b**) Small RNAs isolated from livers of apoB-1 Toc-siRNA-injected mice were probed with siRNA sense strand oligonucleotide in order to examine for the presence of apoB-1 Toc-siRNA antisense strand using northern blotting. The bands for the 21 nucleotides (nt) as well as the 29–30-nt antisense strands were detected. siRNA, short interfering RNA; Toc; α-tocopherol.

Knockdown of target genes in liver and phenotypic analyses of mice using Toc-siRNA

In order to assess the silencing ability of Toc-siRNA *in vivo*, the level of endogenous *apoB* mRNA in the liver was evaluated. The liver was removed 48 hours after the injection and assayed for *apoB* mRNA levels using quantitative reverse transcriptase-polymerase chain reaction (qRT-PCR). The 2 mg/kg apoB-1 Toc-siRNA markedly suppressed *apoB* mRNA when compared with the effect produced by the same volume of maltose, and this silencing effect disappeared when α-tocopherol was not bound to the siRNA. The knockdown effect was specific for the target molecule, as evidenced by the finding that other endogenous mRNAs in the liver, *transthyretin* (*ttr*) and *glyceraldehyde-3-phosphate dehydrogenase* (*gapdh*), did not change, and that a control Toc-siRNA targeting an unrelated gene did not affect them, when mRNA levels were measured relative to total RNA (**Figure 4a**).

Next, we performed a time-course experiment to determine the duration of *apoB* mRNA knockdown effect after single injection of apoB-1 Toc-siRNA. After injection, the reduction of *apoB* mRNA in liver was maximal on day 1 and gradually returned to the baseline level on day 4 (**Figure 4b**). We also performed a dose-response experiment on day 2 after injection. Mice treated with 2, 8, and 32 mg/kg of apoB-1 Toc-siRNA showed significant does-dependent reduction in *apoB* mRNA levels (**Figure 4c**). The intestine, another organ where *apoB* is expressed, was also removed 24 hours after injection and assayed for *apoB* mRNA levels using qRT-PCR. There was no knockdown effect in the intestine as a result of the apoB-1 Toc-siRNA injection (data not shown).

The reduction in liver *apoB* mRNA lowered the export of very low-density lipoprotein (VLDL) from the liver, resulting in a decrease of serum triglyceride (TG) and cholesterol levels and an increase in hepatic lipids.[8] Injection of Toc-siRNA produced significant reduction in TG and cholesterol levels on day 1 (**Figure 5a** and **b**). Further, we performed pathological analysis using Sudan III lipid-staining of liver tissue. The liver sections from mice injected with 2 mg/kg of apoB-1 Toc-siRNA showed a higher number of hepatic lipid droplets than liver sections from control Toc-siRNA-injected mice (**Figure 5c**). Taken together, these results indicate that apoB-1 Toc-siRNA inhibits *apoB* mRNA and alters the phenotype of lipid metabolism in the liver.

No side effects are produced by Toc-siRNA

White blood cell and platelet counts and biochemical analysis of the serum including total protein, aminotransaminases, and blood urea nitrogen after the injection of 2 mg/kg Toc-siRNA (**Table 1**), and pathological analysis of the liver tissue stained with hematoxylin/eosin (data not shown) did not show any marked abnormalities.

The level of induction of interferons (IFNs) was examined at 3 hours (the time interval known to be the IFN phase) after the injection of Toc-siRNA.[5] No IFN-α was detected in the serum (**Table 1**), and RT-PCR of the liver RNA did not amplify *IFN-β*

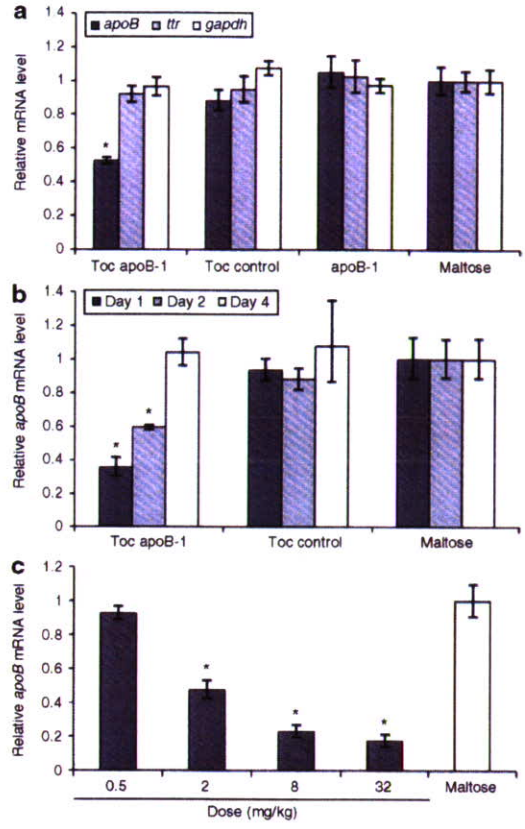

Figure 4 Toc-siRNA-mediated silencing of mouse *apoB* messenger RNA (mRNA) in liver is potent, specific, and dose-dependent. (**a**) The quantitative reverse transcriptase-polymerase chain reaction (qRT-PCR) analyses of several endogenous mRNAs, *apoB, ttr,* and *gapdh* mRNAs in the liver (removed 2 days after injection) relative to total input RNA. $n = 3$, The data shown are mean values ± SEM. $^*P < 0.005$ as compared to the maltose injection group. (**b**) Duration of the gene silencing caused by apoB-1 Toc-siRNA. The qRT-PCR analyses of liver *apoB* mRNA levels relative to *gapdh* mRNA were performed at the indicated time points after injection of apoB-1 Toc-siRNA (Toc apoB-1) or control Toc-siRNA (Toc control). $n = 3$, The data shown are mean values ± SEM. $^*P < 0.005$ as compared to the maltose injection group. (**c**) Dose-dependent reduction of *apoB* mRNA levels in the liver after injection of apoB-1 Toc-siRNA. The *apoB* mRNA levels (normalized to *gapdh* mRNA) were determined 2 days after injection of apoB-1 Toc-siRNA quantitated by qRT-PCR. The data shown are relative to those of mice receiving maltose alone. $n = 3$, The data shown are mean values ± SEM. $^*P < 0.005$ as compared to the maltose injection group. siRNA, short interfering RNA; Toc; α-tocopherol. *gapdh, glyceraldehyde-3-phosphate dehydrogenase; ttr, transthyretin.*

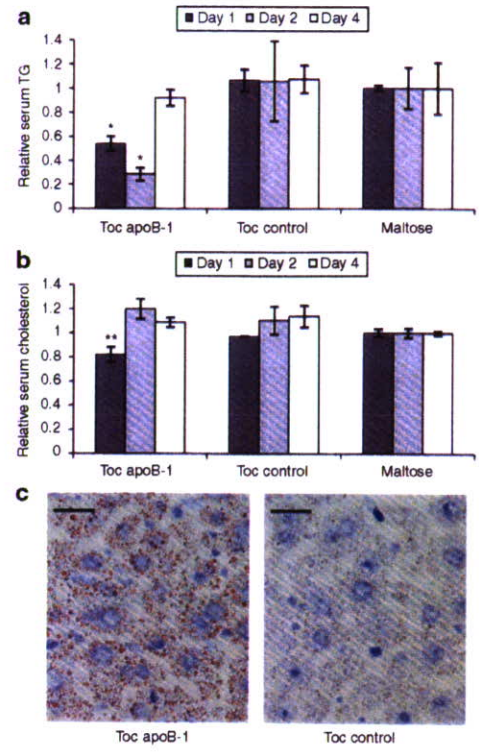

Figure 5 Phenotypic change in lipid metabolism caused by inhibition of liver *apoB* messenger RNA (mRNA). Decreased levels of (**a**) serum triglyceride (TG) and (**b**) cholesterol after knockdown of *apoB* mRNA by apoB-1 Toc-siRNA. Sera were collected from mice before the injections and at 24, 48, and 96 hours after the injections of apoB-1 Toc-siRNA (Toc apoB-1) or control Toc-siRNA (Toc control). The sera were analyzed for TG and cholesterol levels. The values obtained after the injections were divided by those obtained before the injections, and the resultant ratios were normalized to mice which treated with maltose injection. $n = 3$, The data shown are mean values ± SEM. $^*P < 0.01$, $^{**}P < 0.05$ as compared to the maltose injection group. (**c**) Reduction in *apoB* mRNA results in increased hepatic lipid accumulation. Liver sections were prepared 4 days after injection of apoB-1 Toc-siRNA and control Toc-siRNA. The sections were fixed, and lipids were detected by staining with Sudan III. Scale bar = 2 μm. siRNA, short interfering RNA; Toc; α-tocopherol.

mRNA (data not shown). The chemical modifications have been reported as preventing stimulation of Toll-like receptor in the endosomes when siRNA is delivered with cationic liposomes.[20,21] However, the absence of an IFN response to Toc-siRNA does not seem to be the result of chemical modification alone; indeed, a 2 mg/kg dose of Toc-siRNA without chemical modifications also did not induce IFNs (data not shown).

DISCUSSION

We hypothesized that the most effective *in vivo* carrier of siRNA would be a molecule that is essential for target tissue cells but cannot be synthesized within the cells. Vitamins fit these requirements well, and the least toxic of the vitamins even at high doses is vitamin E.[12] Among the eight natural isomers of vitamin E, α- and γ-tocopherol are the most abundant in human diets and are equally well absorbed, but peripheral tissues contain much more of α-tocopherol than of γ-tocopherol,[22] thereby indicating the presence of a selective transport system for α-tocopherol. We therefore planned to use α-tocopherol and its transport system to effect the delivery of siRNA. Because (hydrophilic) siRNA and (lipophilic) α-tocopherol cannot be admixed, we directly bound α-tocopherol molecule to siRNA at the 5′-end of the 29-mer siRNA antisense strand with a phosphate bond (Toc-siRNA) (**Figure 1a** and **b**). We designed 27/29-mer Toc-siRNA with 2 nt 3′-overhang of the antisense strand. The α-tocopherol with 6/8-mer double-strand RNAs is to be cleaved by Dicer in the cytosol, generating the mature form of 21/21-mer siRNA (**Figure 1b**). We actually confirmed, using northern blotting, that the processed 21-mer siRNA antisense strand was detected in mouse liver after injection with Toc-siRNA (**Figure 3b**), and that the binding of

Table 1 IFN-α, BUN, TP, AST, ALT, WBC, and Plt levels in mouse serum after intravenous injection of 2 mg/kg apoB-1 Toc-siRNA or maltose

Treatment		IFN-α (pg/ml)	BUN (mg/dl)	TP (g/dl)	AST (U/l)	ALT (U/l)	WBC (/μl)	Plt (×10⁴/μl)
apoB-1 Toc-siRNA	3 hours	<12.5						
	24 hours		19.1 ± 1.0	5.1 ± 0.1	78 ± 1	21 ± 3	2,800 ± 330	122.0 ± 0.3
	48 hours		24.0 ± 2.4	5.5 ± 0.1	67 ± 4	22 ± 1	2,600 ± 550	112.2 ± 18.9
maltose	3 hours	<12.5						
	24 hours		22.0 ± 0.9	5.5 ± 0.1	79 ± 9	25 ± 2	2,600 ± 560	117.9 ± 13.8
	48 hours		24.5 ± 1.5	5.5 ± 0.1	60 ± 3	26 ± 3	3,700 ± 900	109.0 ± 7.0

Abbreviations: ALT, alanine aminotransferase; AST, aspartate aminotransferase; BUN, blood urea nitrogen; IFN-α, interferon-α; Plt, platelet; TP, total protein; WBC, white blood cell.
The values shown are mean values ± SEM (n = 3).

α-tocopherol did not interfere with the siRNA activity *in vitro* (**Figure 2b**).

This study showed that the binding of α-tocopherol to siRNA enables the efficient *in vivo* delivery of siRNA to the liver. The direct conjugation to siRNA of another lipophilic molecule, cholesterol (Chol-siRNA), was also reported to enhance liver uptake of siRNA.[16] However, the silencing effect produced by Toc-siRNA was more efficient than that by Chol-siRNA, in relation to the identical target gene; much higher doses of Chol-siRNA (50–100 mg/kg) were required for achieving an efficient reduction of *apoB* mRNA in the liver.[4,16] Actually, when cholesterol was conjugated to the same 27/29-mer apoB-1 siRNA with the same chemical modifications as used in apoB-1 Toc-siRNA at the 3′-end of the sense strand, the reduction of *apoB* mRNA induced by 2 mg/kg of this Chol-siRNA was not statistically significant in the livers of mice (data not shown).

The mechanism of uptake of Toc-siRNA by the liver was not elucidated, and the cause of the difference in silencing efficiency between Toc-siRNA and Chol-siRNA is not known. However, there are some possible explanations. First, if α-tocopherol and cholesterol fuse into the lipid bilayer of hepatocyte membrane as cationic liposome does, the difference in hydrophobicity and polarity between α-tocopherol and cholesterol might influence the efficiency of uptake of siRNA by the liver. This cannot be proved, however, because the negative charge of siRNA cannot be cancelled by the addition of α-tocopherol or cholesterol. Moreover, our *in vitro* experiments indicated that Toc-siRNA does not enter the hepatoma culture cell without serum. Second, Toc-siRNA might be incorporated into the serum lipoproteins and enter the hepatocytes via lipoprotein receptors. Recently, Chol-siRNA was shown to use the lipoprotein receptor–mediated pathway to enter hepatocytes.[23] In contrast to cholesterol, α-tocopherol is an exogenous lipid which cannot be synthesized *in vivo*, and therefore the distribution of α-tocopherol among lipoproteins and the mediating receptors in the liver might be different from those of cholesterol. Third, binding of α-tocopherol might enhance uptake of siRNA in the liver by an interacting serum molecule other than lipoprotein. Soutschek and colleagues[16] proposed that the mechanism of Chol-siRNA *in vivo* is related to enhanced binding to serum protein such as albumin. Similarly, α-tocopherol is known to interact with other serum proteins such as SEC14L2, SEC14L3, SEC14L4, and afamin (reviewed in ref. 14).

We observed significant decreases of serum TG and cholesterol and an increase in lipid droplets in the liver after injection of apoB-1 Toc-siRNA. The downregulation of liver ApoB-100 impairs VLDL export and is expected to decrease serum TG as well as cholesterol, because large amounts of TG are incorporated into VLDL particles. This is supported by the fact that the transgenic mouse of truncated *apoB*,[24] and the microsomal TG transfer protein-null mouse,[25,26] neither of which can assemble and secrete VLDL in the liver, show lower serum TG and cholesterol and an accumulation of lipid droplets in the liver. Our results, showing decrease in serum TG as well as in cholesterol, were similar to those of a recent study that used a different siRNA *in vivo* delivery system.[8] Although the decreases in serum TG and cholesterol might be caused by mechanisms other than impaired VLDL export, these results indicate the phenotype of ApoB-100 silencing by Toc-siRNA.

There was no remarkable side effect in blood cell count and biochemical analysis after intravenous injection of Toc-siRNA. The delivered amount of α-tocopherol was only 46 μg/kg when 2 mg/kg Toc-siRNA was injected. This value is very small, considering the need of α-tocopherol as a nutritional element is estimated 10 mg/day for man (125–200 μg/kg/day).[27] In addition, the anti-oxidant activity of α-tocopherol in Toc-siRNA is abolished, because the reactive site of α-tocopherol for anti-oxidation, hydroxyl group at the C6 position, is covalently connected to siRNA (**Figure 1a**). More important, the Toc-siRNA did not induce IFN-α in serum (**Table 1**) and *IFN-β* mRNA in the liver. This absence of adverse side effects associated with the use of Toc-siRNA is important to note, because it is in sharp contrast to the outcome generally described for lipid vector–associated siRNA delivery. The latter is known to produce an immunostimulatory effect,[28] which could cause elevation of transaminases, thrombocytopenia, and lymphopenia.[29] When synthetic lipid–coated siRNA is intravenously injected, it is incorporated in the endosome and then induces IFNs and cytokines through activation of Toll-like receptors located in the endosomal membrane.[20] The possible mechanism of escape from an immunostimulatory effect in Toc-siRNA-injected mice was that Toc-siRNA used the different pathway to enter the cells from synthetic lipid–coated siRNAs. Together, Toc-siRNA is considered to be a noninvasive delivery method of siRNA.

In summary, vitamin E–mediated *in vivo* delivery of siRNA is effective and safe. Although further investigation into the precise delivery pathway of Toc-siRNA is required for better optimization of its use, the findings of this study represent an important step in advancing the use of synthetic siRNA as a very promising system for gene therapy.

MATERIALS AND METHODS

Synthesis of siRNAs. siRNAs were chemically synthesized. In order to combine vitamin E with siRNA, α-tocopherol phosphoramidite was prepared, and then was it connected with the 5′-end of the antisense strand of the siRNA. The DL-α-tocopherol was purchased from Tokyo Kasei, Tokyo, Japan. Synthetic sense and antisense strands of siRNA were then annealed.

Cell culture. Hepa 1-6 cells were maintained in Dulbecco's modified Eagle's medium (Sigma-Aldrich, St Louis, MO) only, or supplemented with 10% fetal bovine serum (Invitrogen, Carlsbad, CA), 100 U/ml penicillin, and 100 μg of streptomycin at 37 °C in 5% CO_2.

qRT-PCR. Total RNA was extracted from the culture cells or mice liver using Isogen (Nippon Gene, Tokyo, Japan). The RNA was reverse transcribed with Superscript III and random hexamers (Invitrogen, Carlsbad, CA). The qRT-PCR was performed on 1.5 μg of complementary DNA using the TaqMan Universal PCR Master Mix (Applied Biosystems, Foster City, CA) in accordance with the manufacturer's instructions. The amplification conditions were 40 cycles of denaturation at 95 °C for 15 seconds and annealing at 60 °C for 60 seconds with ABI PRISM 7700 Sequence Detector. Primers for mouse *apoB*, *gapdh*, *ttr*, and *IFN-β* mRNAs were designed by Applied Biosystems (Foster City, CA).

In vitro *activity and stability assays.* In order to determine *in vitro* activity of siRNAs, Hepa 1-6 cells were transfected with 10 nmol/l of siRNAs using Lipofectamine RNAiMAX (Invitrogen, Carlsbad, CA), or transfected with 2 μmol/l of Toc-siRNAs without any transfection reagents. The cells were harvested 24 hours after transfection. Total RNA was extracted and the amount of endogenous *apoB* mRNA was measured using qRT-PCR.

In order to study the stability of the siRNAs in serum, (i) siRNA with both strands naked, (ii) siRNA with both strands modified, (iii) siRNA with only the sense strand modified, (iv) Toc-siRNA with both strands naked, and (v) Toc-siRNA with both strands modified (100 pmol each) were incubated at 37 °C in mouse serum for 4, 8, 16, and 24 hours. Aliquots taken at different time points were treated with Proteinase K (Wako Pure Chemical Industries, Osaka, Japan) and frozen in urea Tris-buffered electrophoresis-loading buffer. All samples were subjected to electrophoresis on 2% agarose gels.

Northern blotting. Total RNA was extracted from mice liver using MirVana (Ambion, Austin, TX). Total RNA was condensed with Ethachinmate (Nippon gene) and 2 μg of RNA was separated by electrophoresis on a 14% polyacrylamide-urea gel and transferred to a Hybond-N^+ membrane (Amersham Biosciences, Piscataway, NJ). The blot was hybridized with a probe of the siRNA antisense sequence which was labeled with fluorescein using Gene Images 3′-Oligolabelling kit (Amersham Biosciences, Piscataway, NJ). The signals were visualized by Gene Images CDP-star detection Kit (Amersham Biosciences, Piscataway, NJ).

Pathological analysis. For pathological analysis of side effects by Toc-siRNA, the liver sample was postfixed in 4% paraformaldehyde/phosphate-buffered saline solution for 6 hour and embedded in paraffin, sectioned at 4-μm thick using a Leica CM 3050 S cryostat (Leica Microsystems, Wetzlar, Germany), and then stained with hematoxylin/eosin.

To analyze of liver lipid accumulation, liver samples from apoB-1 and control Toc-siRNA-treated mice were sectioned (4 μm) and fixed in 4% paraformaldehyde/phosphate-buffered saline for 5 minutes, and then stained with filtrated Sudan III (Muto Pure Chemicals, Tokyo, Japan) 37 °C for 30 minutes. Counterstaining of nuclei was performed with Mayer hematoxylin solution (Muto Pure Chemicals, Tokyo, Japan) for 3 minutes.

For pathological analysis of delivery of siRNA to liver, 8 mg/kg Cy3-labeled siRNA with or without α-tocopherol within 0.25 ml of 10% maltose was injected from the tail vein of ICR mouse. One hour after intravenous injection, mouse was killed and liver samples were harvested. Liver samples were fixed in 4% paraformaldehyde/phosphate-buffered saline for 6 hour. Fixed tissue samples were snap-frozen in liquid nitrogen. Frozen tissue sections were prepared and stained with 13 nmol/l Alexa-488 phalloidin (Invitrogen, Carlsbad, CA). The slides were analyzed using LSM 510 confocal microscope (Carl Zeiss MicroImaging, Oberkochen, Germany). Each image comprised a flattened projection of 11 optical images (0.4 μm each) to represent combined fluorescence signals from a 4-μm thick section.

Statistical analysis. Student's *t*-test was used to evaluate differences between siRNA-transfected groups and cells alone *in vitro*, and between Toc-siRNA-injected groups and maltose only injected group *in vivo*.

ACKNOWLEDGMENTS

We thank Tadaaki Ohgi, Nippon Shinyaku, for his technical support. This work was supported by grants from the Ministry of Education, Science and Culture, Japan (#18650103) and the Ministry of Health Labor and Welfare, Japan (#2212065), and a grant from the 21st Century Center of Excellence Program on Brain Integration and its Disorders given to Tokyo Medical and Dental University.

REFERENCES

1. Davidson, BL and Harper, SQ (2005). Viral delivery of recombinant short hairpin RNAs. *Methods Enzymol* **392**: 145–173.
2. McCaffrey, AP, Meuse, L, Pham, TT, Conklin, DS, Hannon, GJ and Kay, MA (2002). RNA interference in adult mice. *Nature* **418**: 38–39.
3. Hino, T, Yokota, T, Ito, S, Nishina, K, Kang, YS, Mori, S *et al.* (2006). *In vivo* delivery of small interfering RNA targeting brain capillary endothelial cells. *Biochem Biophys Res Commun* **340**: 263–267.
4. Zimmermann, TS, Lee, AC, Akinc, A, Bramlage, B, Bumcrot, D, Fedoruk, MN *et al.* (2006). RNAi-mediated gene silencing in non-human primates. *Nature* **441**: 111–114.
5. Yokota, T, Iijima, S, Kubodera, T, Ishii, K, Katakai, Y, Ageyama, N *et al.* (2007). Efficient regulation of viral replication by siRNA in a non-human primate surrogate model for hepatitis C. *Biochem Biophys Res Commun* **361**: 294–300.
6. Spagnou, S, Miller, AD and Keller, M (2004). Lipidic carriers of siRNA: differences in the formulation, cellular uptake, and delivery with plasmid DNA. *Biochemistry* **43**: 13348–13356.
7. Baigude, H, McCarroll, J, Yang, CS, Swain, PM and Rana, TM (2007). Design and creation of new nanomaterials for therapeutic RNAi. *ACS Chem Biol* **2**: 237–241.
8. Rozema, DB, Lewis, DL, Wakefield, DH, Wong, SC, Klein, JJ, Roesch, PL *et al.* (2007). Dynamic PolyConjugates for targeted *in vivo* delivery of siRNA to hepatocytes. *Proc Natl Acad Sci USA* **104**: 12982–12987.
9. Sato, A, Takagi, M, Shimamoto, A, Kawakami, S and Hashida, M (2007). Small interfering RNA delivery to the liver by intravenous administration of galactosylated cationic liposomes in mice. *Biomaterials* **28**: 1434–1442.
10. Kim, SI, Shin, D, Choi, TH, Lee, JC, Cheon, GJ, Kim, KY *et al.* (2007). Systemic and specific delivery of small interfering RNAs to the liver mediated by apolipoprotein A-I. *Mol Ther* **15**: 1145–1152.
11. Kumar, P, Wu, H, McBride, JL, Jung, KE, Kim, MH, Davidson, BL *et al.* (2007). Transvascular delivery of small interfering RNA to the central nervous system. *Nature* **448**: 39–43.
12. Kappus, H and Diplock, AT (1992). Tolerance and safety of vitamin E: a toxicological position report. *Free Radic Biol Med* **13**: 55–74.
13. Rigotti, A (2007). Absorption, transport, and tissue delivery of vitamin E. *Mol Aspects Med* **28**: 423–436.
14. Zingg, JM (2007). Vitamin E: an overwiew of major research directions. *Mol Aspects Med* **28**: 400–422.
15. Rose, SD, Kim, DH, Amarzguioui, M, Heidel, JD, Collingwood, MA, Davis, ME *et al.* (2005). Functional polarity is introduced by Dicer processing of short substrate RNAs. *Nucleic Acids Res* **33**: 4140–4156.
16. Soutschek, J, Akinc, A, Bramlage, B, Charisse, K, Constien, R, Donoghue, M *et al.* (2004). Therapeutic silencing of an endogenous gene by systemic administration of modified siRNAs. *Nature* **432**: 173–178.
17. Chiu, YL and Rana, TM (2003). siRNA function in RNAi: a chemical modification analysis. *RNA* **9**: 1034–1048.
18. Czauderna, F, Fechtner, M, Dames, S, Aygün, H, Klippel, A, Pronk, GJ *et al.* (2003). Structural variations and stabilising modifications of synthetic siRNAs in mammalian cells. *Nucleic Acids Res* **31**: 2705–2716.
19. Miyoshi, K, Tsukumo, H, Nagami, T, Siomi, H and Siomi, MC (2005). Slicer function of *Drosophila* Argonautes and its involvement in RISC formation. *Genes Dev* **19**: 2837–2848.
20. Judge, AD, Bola, G, Lee, AC and MacLachlan, I (2006). Design of noninflammatory synthetic siRNA mediating potent gene silencing *in vivo*. *Mol Ther* **13**: 494–505.
21. Sioud, M, Furset, G and Cekaite, L (2007). Suppression of immunostimulatory siRNA-driven innate immune activation by 2′-modified RNAs. *Biochem Biophys Res Commun* **361**: 122–126.

22. Aftergood, L and Alfin-Slater, RB (1978). Effect of administration of α- and γ-tocopherol on tissue distribution and red cell hemolysis in rats. *Int J Vitam Nutr Res* **48**: 32–37.
23. Wolfrum, C, Shi, S, Jayaprakash, KN, Jayaraman, M, Wang, G, Pandey, RK *et al.* (2007). Mechanisms and optimization of *in vivo* delivery of lipophilic siRNAs. *Nat Biotechnol* **25**: 1149–1157.
24. Chen, Z, Fitzgerald, RL, Averna, MR and Schonfeld, G (2000). A targeted apolipoprotein B-38.9-producing mutation causes fatty livers in mice due to the reduced ability of apolipoprotein B-38.9 to transport triglycerides. *J Biol Chem* **275**: 32807–32815.
25. Raabe, M, Véniant, MM, Sullivan, MA, Zlot, CH, Björkegren, J, Nielsen, LB *et al.* (1999). Analysis of the role of microsomal triglyceride transfer protein in the liver of tissue-specific knockout mice. *J Clin Invest* **103**: 1287–1298.
26. Minehira-Castelli, K, Leonard, SW, Walker, QM, Traber, MG and Young, SG (2006). Absence of VLDL secretion does not affect α-tocopherol content in peripheral tissues. *J Lipid Res* **47**: 1733–1738.
27. Food and Nutrition Board, National Academy of Sciences, National Research Council (1989). *Recommended Dietary Allowances* 10th edn. National Academy Press: Washington, DC, pp 99–107.
28. Robbins, M, Judge, A, Liang, L, McClintock, K, Yaworski, E and MacLachlan, I (2007). 2′-O-methyl-modified RNAs act as TLR7 antagonists. *Mol Ther* **15**: 1663–1669.
29. Morrissey, DV, Lockridge, JA, Shaw, L, Blanchard, K, Jensen, K, Breen, W *et al.* (2005). Potent and persistent *in vivo* anti-HBV activity of chemically modified siRNAs. *Nat Biotechnol* **23**: 1002–1007.

doi:10.1111/j.1440-1746.2007.05076.x

HEPATOLOGY

Inhibition of hepatitis C virus infection and expression *in vitro* and *in vivo* by recombinant adenovirus expressing short hairpin RNA

Naoya Sakamoto,*,† Yoko Tanabe,* Takanori Yokota,‡ Kenichi Satoh,§ Yuko Sekine-Osajima,* Mina Nakagawa,*,† Yasuhiro Itsui,* Megumi Tasaka,* Yuki Sakurai,* Chen Cheng-Hsin,* Masahiko Yano,¶ Shogo Ohkoshi,¶ Yutaka Aoyagi,¶ Shinya Maekawa,†† Nobuyuki Enomoto,†† Michinori Kohara§ and Mamoru Watanabe*

Departments of *Gastroenterology and Hepatology, †Hepatitis Control, and ‡Neurology and Neurological Science, Tokyo Medical and Dental University, §Department of Microbiology and Cell Biology, The Tokyo Metropolitan Institute of Medical Science, Tokyo, ¶Gastroenterology and Hepatology Division, Graduate School of Medical and Dental Sciences, Niigata University, Niigata, and ††First Department of Medicine, Yamanashi University, Yamanashi, Japan

Key words
adenovirus vector, hepatitis C virus, RNA interference.

Accepted for publication 12 April 2007.

Correspondence
Dr Naoya Sakamoto, Department of Gastroenterology and Hepatology, Tokyo Medical and Dental University, 1-5-45 Yushima, Bunkyo-ku, Tokyo 113-8519, Japan.
Email: nsakamoto.gast@tmd.ac.jp

NS and YT have contributed equally to this paper.

Abstract

Background and Aim: We have reported previously that synthetic small interfering RNA (siRNA) and DNA-based siRNA expression vectors efficiently and specifically suppress hepatitis C virus (HCV) replication *in vitro*. In this study, we investigated the effects of the siRNA targeting HCV-RNA *in vivo*.

Methods: We constructed recombinant retrovirus and adenovirus expressing short hairpin RNA (shRNA), and transfected into replicon-expressing cells *in vitro* and transgenic mice *in vivo*.

Results: Retroviral transduction of Huh7 cells to express shRNA and subsequent transfection of an HCV replicon into the cells showed that the cells had acquired resistance to HCV replication. Infection of cells expressing the HCV replicon with an adenovirus expressing shRNA resulted in efficient vector delivery and expression of shRNA, leading to suppression of the replicon in the cells by ~10^{-3}. Intravenous delivery of the adenovirus expressing shRNA into transgenic mice that can be induced to express HCV structural proteins by the Cre/*lox*P switching system resulted in specific suppression of virus protein synthesis in the liver.

Conclusion: Taken together, our results support the feasibility of utilizing gene targeting therapy based on siRNA and/or shRNA expression to counteract HCV replication, which might prove valuable in the treatment of hepatitis C.

Introduction

Hepatitis C virus (HCV), which affects 170 million people worldwide, is one of the most important pathogens causing liver-related morbidity and mortality.[1] The difficulty in eradicating HCV is attributable to limited treatment options against the virus and their unsatisfactory efficacies. Even with the most effective regimen with pegylated interferon (IFN) and ribavirin in combination, the efficacies are limited to less than half of the patients treated.[2] Given this situation, the development of safe and effective anti-HCV therapies is one of our high-priority goals.

RNA interference (RNAi) is a process of sequence-specific, post-transcriptional gene silencing that is initiated by double-stranded RNA.[3,4] Because of its potency and specificity, RNAi rapidly has become a powerful tool for basic research to analyze gene functions and for potential therapeutic applications. Recently, successful suppression of various human pathogens by RNAi have been reported, including human immunodeficiency viruses,[5,6] poliovirus,[7] influenza virus,[8] severe acute respiratory syndrome (SARS) virus[9] and hepatitis B virus (HBV).[10–13]

We and other researchers have reported that appropriately designed small interfering RNA (siRNA) targeting HCV genomic RNA can efficiently and specifically suppress HCV replication *in vitro*.[14–19] We have tested siRNA designed to target the well-conserved 5′-untranslated region (5′-UTR) of HCV-RNA, and identified the most effective target, just upstream of the translation initiation codon. Furthermore, transfection of DNA-based vectors expressing siRNA was as effective as that of synthetic siRNA in suppressing HCV replication.[14]

In this study, we explored the further possibility that efficient delivery and expression of siRNA may be effective in suppression and elimination of HCV replication and that delivery of such

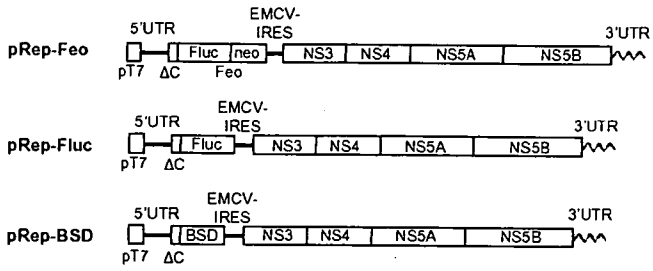

Figure 1 Structures of HCV replicon plasmids. The pRep-Feo expressed a chimeric reporter protein of firefly luciferase (Fluc) and neomycin phosphotransferase (GenBank accession No. AB119282).[14,20] The pRep-Fluc expressed the Fluc protein. The pRep-BSD expressed the blasticidin S (BSD) resistance gene. pT7, T7 promoter; 5'UTR, HCV 5'-untranslated region; ΔC, truncated HCV core region (nt. 342–377); neo, neomycin phosphotransferase gene; EMCV, encephalomyocarditis virus; NS3, NS4, NS5A and NS5B, genes that encode HCV non-structural proteins; 3'UTR, HCV 3'-untranslated region.

HCV-directed siRNA *in vivo* may be effective in silencing viral protein expression in the liver. Here, we report that HCV replication was suppressed *in vitro* by recombinant retrovirus and adenovirus vectors expressing short hairpin RNA (shRNA) and that the delivery of the adenovirus vector to mice *in vivo* specifically inhibited viral protein synthesis in the liver.

Methods

Cells and cell culture

Huh7 and Retro Pack PT67 cells (Clontech, Palo Alto, CA, USA) were maintained in Dulbecco's modified minimal essential medium (Sigma, St. Louis, MO, USA) supplemented with 10% fetal calf serum at 37°C under 5% CO_2. To maintain cell lines carrying the HCV replicon, G418 (Wako, Osaka, Japan) was added to the culture medium to a final concentration of 500 μg/mL.

HCV replicon constructs and transfection

HCV replicon plasmids, pRep-Feo, pRep-Fluc and pRep-BSD were constructed from were constructed from a virus, HCV-N strain, genotype 1b.[21] The pRep-Feo expressed a chimeric reporter protein of firefly luciferase (Fluc) and neomycin phosphotransferase.[14,20] The pRep-Fluc and the pRep-BSD expressed the Fluc and blasticidin S (BSD) resistance genes, respectively (Fig. 1). The replicon RNA synthesis and the transfection protocol have been described previously.[22]

Synthetic siRNA and siRNA-expression plasmid

The design and construction of HCV-directed siRNA vectors have been described.[14] Briefly, five siRNA targeting the 5'-UTR of HCV RNA were tested for their efficiency to inhibit HCV replication, and the most effective sequence, which targeted nucleotide position of 331 though 351, was used in the present study. To construct shRNA-expressing DNA cassettes, oligonucleotide inserts were synthesized that contained the loop sequence (5'-TTC AAG AGA-3') flanked by sense and antisense siRNA sequences (Fig. 2a). These were inserted immediately downstream of the human U6 promoter. To avoid a problem in transcribing shRNA because of instability of the DNA strands arising from the tight palindrome structure, several C-to-T point mutations, which retained completely the silencing activity of the shRNA, were introduced into the sense strand of the shRNA sequences (referred to as 'm').[23] A control plasmid, pUC19-shRNA-Control, expressed shRNA directed towards the Machado–Joseph disease gene, which is a mutant of ataxin-3 gene and is not normally expressed. We have previously described the sequence specific activity of the shRNA-Control.[24]

Prior to construction of the virus vectors, we tested silencing efficiency of five shRNA constructs of different lengths that covered the target sequence (Fig. 2a). The shRNA-HCV-19, shRNA-HCV-21 and shRNA-HCV-27 had target sequences of 19, 21 and 27 nucleotides, respectively. Transfection of these shRNA constructs into Huh7/pRep-Feo showed that shRNA with longer target sequences had better suppressive effects (Fig. 2b). Therefore, we used shRNA-HCV-27m (abbreviated as shRNA-HCV) in the following study.

Recombinant retrovirus vectors

The U6-shRNA expression cassettes were inserted into the *StuI*/*Hin*dIII site of a retrovirus vector, pLNCX2 (Clontech) to construct pLNCshRNA-HCV and pLNCshRNA-Control (Fig. 2c). The plasmids were transfected into the packaging cells, Retro Pack PT67. The culture supernatant was filtered and added onto Huh7 cells with 4 μg/mL of polybrene. Huh7 cell lines stably expressing shRNA were established by culture in the presence of 500 μg/mL of G418.

Recombinant adenovirus

Recombinant adenoviruses expressing shRNA were constructed using an Adenovirus Expression Vector Kit (Takara, Otsu, Japan). The U6-shRNA expression DNA cassette was inserted into the *SwaI* site of pAxcw to construct pAxshRNA-HCV and pAxshRNA-Control. The adenoviruses were propagated according to the manufacturer's protocol (AxshRNA-HCV and AxshRNA-Control; Fig. 2c). A 'multiplicity of infection' (MOI) was used to standardize infecting doses of adenovirus. The MOI stands for the ratio of infectious virus particles to the number of cells being infected. An MOI = 1 represents equivalent dose to introduce one infectious virus particle to every host cell that is present in the culture.

Plasmids for assays of interferon responses

pISRE-TA-Luc (Invitrogen, Carlsbad, CA, USA) contained five copies of the consensus interferon stimulated response element (ISRE) motifs upstream of the Fluc gene. pTA-Luc (Invitrogen), which lacks the enhancer element, was used for background determination. The pcDNA3.1 (Invitrogen) was used as an empty vector for mock transfection. pRL-CMV (Promega, Madison, WI, USA), which expresses the *Renilla* luciferase protein, was used for normalization of transfection efficiency.[25] A plasmid, peGFPneo (Invitrogen), was used to monitor percentages of transduced cells.

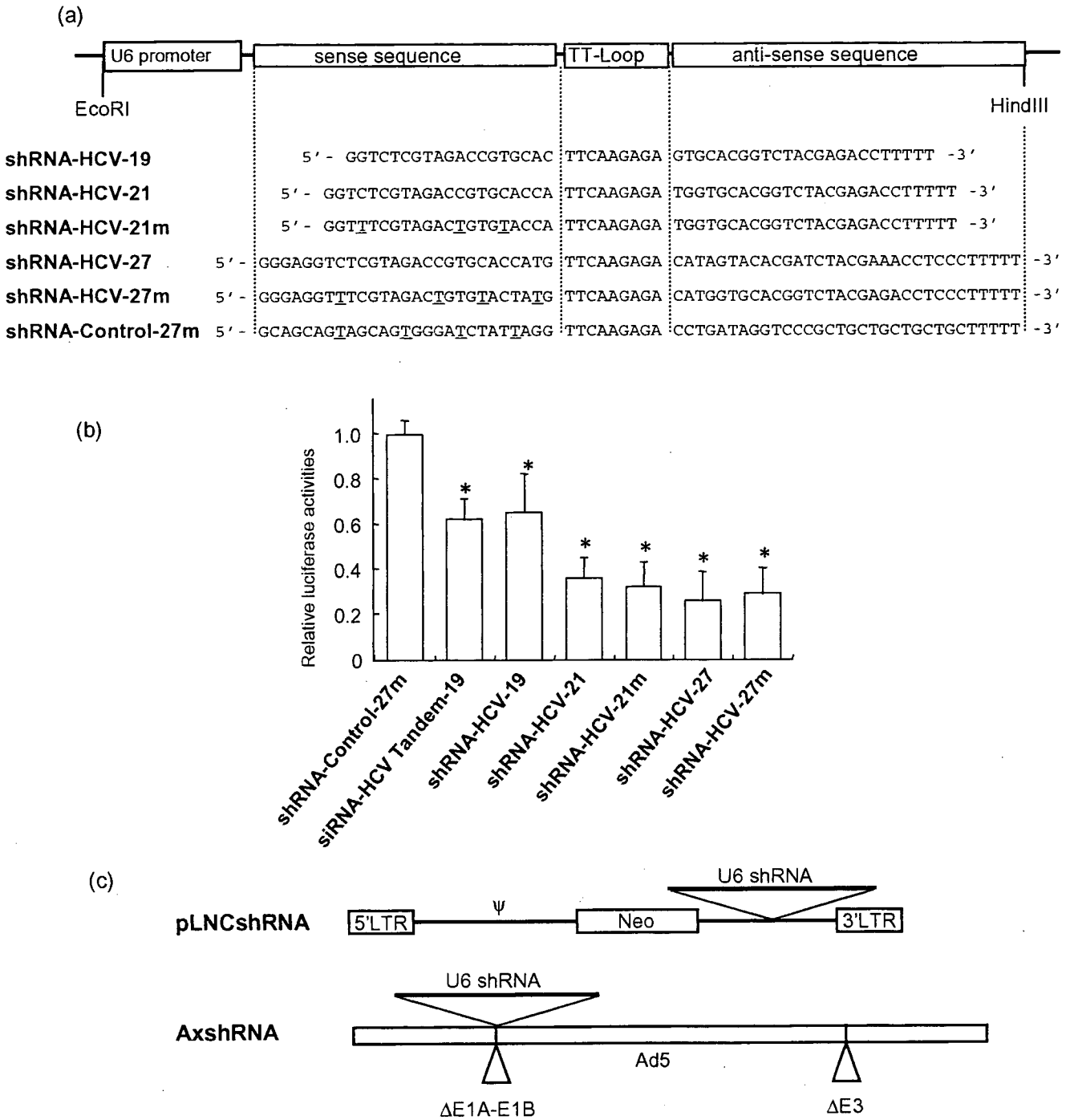

Figure 2 Structure of shRNA-expression constructs and shRNA sequences. (a) Structure of shRNA-expression cassette and shRNA sequences. TT-Loop, the loop sequence. The shRNA-Control was directed toward an unrelated target, Machado–Joseph disease gene. Underlined letters indicate C-to-T point mutations in the sense strand. (b) The shRNA-expression plasmids were transfected into Huh7/pRep-Feo cells, and internal luciferase activities were measured at 48 h of transfection. Each assay was done in triplicate, and the values are displayed as mean + SD. $^*P < 0.05$. (c) pLNCshRNA, structure of a recombinant retrovirus expressing shRNA. Ψ, the retroviral packaging signal sequence. AxshRNA, structure of a recombinant adenovirus expressing shRNA.

Real-time RT-PCR analysis

Total cellular RNA was extracted from cultured cells or liver tissue using ISOGEN (Nippon Gene, Tokyo, Japan). Total cellular RNA (2 μg) was used to generate cDNA from each sample using the SuperScript II reverse-transcriptase (Invitrogen). The mRNA expression levels were measured using the Light Cycler PCR and detection system (Roche, Mannheim, Germany) and Light Cycler Fast Start DNA Master SYBR Green 1 mix (Roche).

Luciferase assays

Luciferase activity was measured using a luminometer, Lumat LB9501 (Promega) and the Bright-Glo Luciferase Assay System (Promega) or the Dual-Luciferase Reporter Assay System (Promega).

Northern and western hybridization

Total cellular RNA was separated by denaturing agarose-formaldehyde gel electrophoresis, and transferred to a nylon membrane. The membrane was hybridized with a digoxigenin-labeled probe specific for the full-length replicon sequence, and subsequently with a probe specific for beta-actin. The signals were detected by chemiluminescence reaction using a Digoxigenin Luminescent Detection Kit (Roche), and visualized by Fluoro-Imager (Roche). For the western blotting, 10 μg of total cell lysate was separated on NuPAGE 4.12% Bis-TrisGel (Invitrogen), and blotted onto an Immobilon PVDF Membrane (Roche). The membrane was incubated with monoclonal antibodies specific for HCV-NS5A (BioDesign, Saco, ME, USA), NS4A (Virogen, Watertown, MA, USA), or beta-actin (Sigma), and detected by a chemiluminescence reaction (BM Chemiluminescence Blotting Substrate; POD, Roche).

Transient-replication assays

A replicon, pRep-Fluc, was transfected into cells and the luciferase activities of the cell lysates were measured serially. To correct the transfection efficiency, each value was divided by the luciferase activity at 4 h after the transfection.

Stable colony formation assays

Cells were transfected with a replicon, pRep-BSD, and were cultured in the presence of 150 μg/mL of BSD (Invitrogen). BSD-resistant cell colonies appeared after ~3 weeks of culture, and were counted.

HCV-JFH1 virus cell culture

An *in-vitro* transcribed HCV-JFH1 RNA[26] was transfected into Huh7.5.1 cells.[27] Naive Huh7.5.1 cells were subsequently infected by the culture supernatant of the JFH1-RNA transfected Huh-7.5.1 cells, and subjected to siRNA or drug treatments. Replication levels of HCV-RNA were quantified by the realtime RT-PCR by using primers that targeted HCV-NS5B region, HCV-JFH1 sense: 5′-TCA GAC AGA GCC TGA GTC CA-3′, and HCV-JFH1 antisense: 5′-AGT TGC TGG AGG GCT TCT GA-3′.

Mice and adenovirus infection

Transgenic mice, CN2-29, inducibly express mRNA for the HCV structural proteins (genotype1b, nucleotides 294–3435) by the Cre/*lox*P switching system.[28] The transgene does not contain full-length HCV 5′-UTR, but shares the target sequence of the shRNA-HCV. Although the transgenic mouse CN2 has been previously reported as expressing higher levels of the viral proteins, the expression levels of the viral core protein in the CN2-29 mice are modest and similar to that in the liver of HCV patients. Thus, we chose CN2-29 mice in the present study.

The mice were infected with AxshRNA-HCV or controls (AxshRNA-Control or AxCAwl) in combination with AxCAN-Cre, which expressed Cre recombinase. Three days after the infection, the mice were killed and HCV core protein in the liver was measured as described below. The BALB/c mice were maintained in the Animal Care Facility of Tokyo Medial and Dental University, and transgenic mice were in the Tokyo Metropolitan Institute of Medical Science. Animal care was in accordance with institutional guidelines. The review board of the university approved our experimental animal studies and all experiments were approved by the institutional animal study committees.

Measurement of HCV core protein in mouse liver

The amounts of HCV core protein in the liver tissue from the mice was measured by a fluorescence enzyme immunoassay (FEIA)[29] with a slight modification. Briefly, the 5F11 monoclonal anti-HCV-core antibody was used as the first antibody on the solid phase, and the 5E3 antibody conjugated with horseradish peroxidase was the second antibody. This FEIA can detect as little as 4 pg/mL of recombinant HCV-core protein. Contents of the HCV core protein in the liver samples were normalized by the total protein contents and expressed as pg/mg total protein.

Immunohistochemical staining

Liver tissue was frozen with optimal cutting temperature (OTC) compound (Tissue Tek; Sakura Finetechnical, Tokyo, Japan). The sections (8 μm thick) were fixed with a 1:1 solution of acetone : methanol at −20°C for 10 min and then washed with phosphate-buffered saline (PBS). Subsequently, the sections were incubated with the IgG fraction of an anti-HCV core rabbit polyclonal antibody (RR8)[28] in blocking buffer or antialbumin rabbit polyclonal antibody (Dako Cytomation, Glostrup, Denmark) in PBS overnight at 4°C. The sections were incubated with secondary antibody, Alexa-antirabbit IgG (Invitrogen) or TRITIC-antirabbit IgG (Sigma), for 2 h at room temperature. Fluorescence was observed using a fluorescence microscope.

Statistical analyses

Statistical analyses were performed using Student's *t*-test; *P*-values of less than 0.05 were considered to be statistically significant.

Results

Retrovirus transduction of shRNA can protect from HCV replication

Retrovirus vectors propagated from pLNCshRNA-HCV and pLNCshRNA-Control were used to infect Huh7 cells, and cell lines were established that constitutively express shRNA-HCV and shRNA-Control (Huh7/shRNA-HCV and Huh7/shRNA-Control, respectively). There were no differences in the cell morphology or growth rate between shRNA-transduced and non-transduced Huh7 cells (data not shown). The HCV replicon, pRep-Fluc, was transfected into Huh7/shRNA-HCV, Huh7/shRNA-Control and naive Huh7 cells by electroporation. In Huh7/shRNA-Control and naive Huh7 cells, the initial luciferase activity at 4 h decreased temporarily, which represents decay of the transfected replicon RNA, but increased again at 48 h and 72 h, which demonstrate de novo synthesis of the HCV replicon RNA. In contrast, transfection into Huh7/shRNA-HCV cells resulted in a decrease in the initial luciferase activity, reaching background by 72 h (Fig. 3a). Similarly, transfection of the replicon, pRep-BSD, into Huh7 cells and BSD selection yielded numerous BSD-resistant colonies in the naive Huh7 (832 colonies) and Huh7/shRNA-Control cell lines (740 colonies), while transfection of Huh7/shRNA-HCV, which expressed shRNA-HCV, yielded obviously fewer colonies (five colonies), indicating reduction of colony forming units by ~10^2 (Fig. 3b). There was no difference in shape, growth or viability between cells expressing the shRNA or not. These results indicated that cells expressing HCV-directed shRNA following retrovirus transduction acquired resistance to HCV replication.

Effect of recombinant adenoviruses expressing shRNA on *in vitro* HCV replication

We investigated subsequently the effects of recombinant adenovirus vectors expressing shRNA. AxshRNA-HCV and AxshRNA-Control were used separately to infect Huh7/pRep-Feo cells, and the internal luciferase activities were measured sequentially (Fig. 4a). AxshRNA-HCV caused continuous suppression of HCV RNA replication. Six days postinfection, the luciferase activities fell to background levels. In contrast, the luciferase activities of the Huh7/pRep-Feo cells infected with AxshRNA-Control did not show any significant changes compared with untreated Huh7/pRep-Feo cells (Fig. 4a). The dimethylthiazol carboxymethoxyphenyl sulfophenyl tetrazolium (MTS) assay showed no significant difference between cells that were infected by recombinant adenovirus and uninfected cells (Fig. 4b). In the northern blotting analysis, the cells were harvested 6 days after infection with the adenovirus at an MOI of 1. Feo-replicon RNA of 9.6 kb, which was detectable in the untreated Huh7/pRep-Feo cells and in the cells infected with AxshRNA-Control, diminished substantially following infection with the AxshRNA-HCV (Fig. 4c). Densitometries showed that the intracellular levels of the replicon RNA in the Huh7/pRep-Feo cells correlated well with the internal luciferase activities. Similarly in the western blotting, cells were harvested 6 days after infection with adenovirus. Levels of the HCV NS4A and NS5A proteins that were translated from the HCV replicon decreased following infection with the AxshRNA-HCV

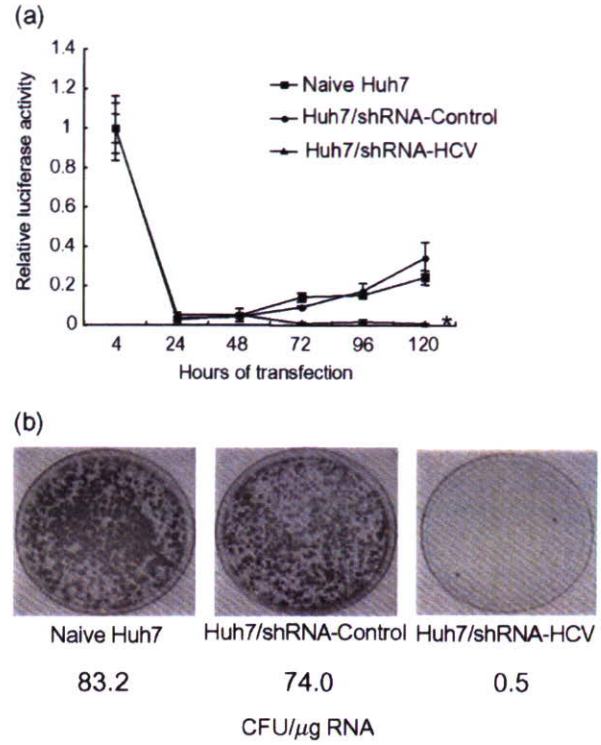

Figure 3 HCV replication can be inhibited by shRNA-HCV which was stably transfected into cells. Huh7/shRNA-HCV and Huh7/shRNA-Control stably express shRNA-HCV or shRNA-Control, respectively, following retroviral transduction. (a) Transient replication assay. An HCV replicon RNA, pRep-Fluc, was transfected into naive Huh7, Huh7/shRNA-HCV and Huh7/shRNA-Control cells. Luciferase activities of the cell lysates were measured serially at the times indicated, and the values were plotted as ratios relative to luciferase activities at 4 h. The luciferase activities at 4 h represent transfected replicon RNA. The data are mean ± SD. An asterisk denotes a *P*-value of less than 0.001 compared with the corresponding value of the naive Huh7 cells. (b) Stable colony formation assay. The HCV replicon, pRep-BSD, was transfected into naive Huh7, Huh7/shRNA-HCV and Huh7/shRNA-Control cells. The cells were cultured in the presence of blasticidin S (BSD) in the medium for ~3 weeks, and the BSD-resistant colonies were counted. These assays were repeated twice. The colony-forming units per microgram RNA (CFU/μg RNA) are shown at the bottom.

(Fig. 4d). These results indicated that the decrease in luciferase activities was due to specific suppressive effects of shRNA on expression of HCV genomic RNA and the viral proteins, and not due to non-specific effects caused by the delivery of shRNA or to toxicity of the adenovirus vectors.

Absence of interferon-stimulated gene responses by siRNA delivery

It has been reported that double-stranded RNA may induce interferon-stimulated gene (ISG) responses which cause instability of mRNA, translational suppression of proteins and apoptotic cell

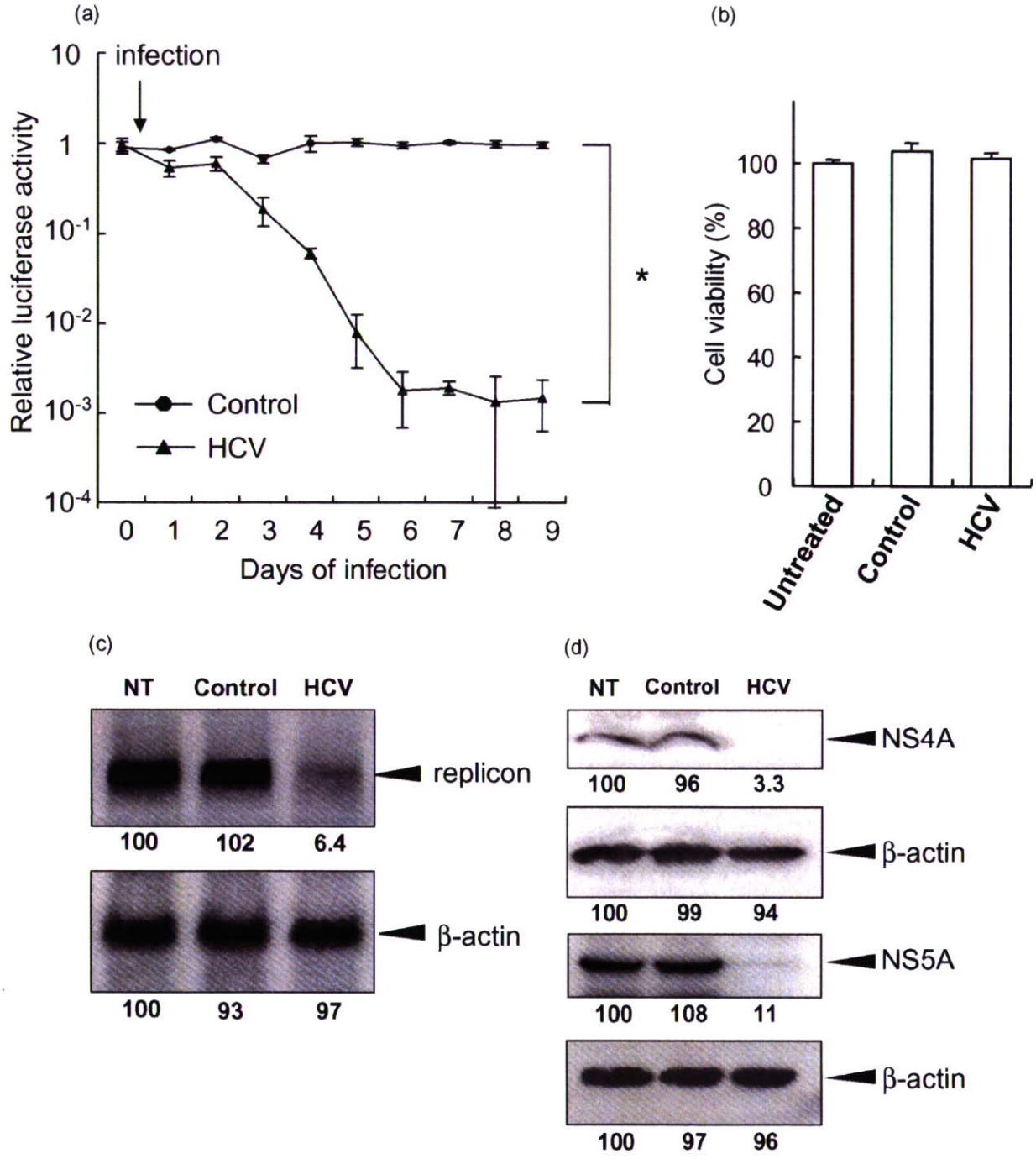

death.[18,30,31] Therefore, we examined the effects of the shRNA-expressing plasmids and adenoviruses on the activation of ISG expression in cells. The ISRE-reporter plasmid, pISRE-TA-Luc, and a control plasmid, peGFPneo, were transfected into Huh7 cells with plasmid pUC19-shRNA-HCV or pUC19-shRNA-Control, or adenovirus, AxshRNA-HCV or AxshRNA-Control, and the ISRE-mediated luciferase activities were measured. On day 2, the ISRE-luciferase activities did not significantly change in cells in which

Figure 4 Effect of a recombinant adenovirus expressing shRNA on HCV replicon. (a) Huh7/pRep-Feo cells were infected with AxshRNA-HCV or shRNA-Control at a multiplicity of infection (MOI) of 1. The cells were harvested, and internal luciferase activities were measured on day 0 though day 9 after adenovirus infection. Each assay was done in triplicate, and the value is displayed as a percentage of no treatment and as mean ± SD. An asterisk indicates a *P*-value of less than 0.05. (b) Dimethylthiazol carboxymethoxyphenyl sulfophenyl tetrazolium (MTS) assay of Huh7/pRep-Feo cells. Cells were infected with indicated recombinant adenoviruses at an MOI of 1. The assay was done at day 6 of infection. Error bars indicate mean + SD. (c) Northern blotting. The upper panel shows replicon RNA, and the lower panel shows beta-actin mRNA. (d) Western blotting. Total cell lysates were separated on NuPAGE gel, blotted and incubated with monoclonal anti-NS4A or anti-NS5A antibodies. The membrane was re-blotted with antibeta-actin antibodies. NT, untreated Huh7/pRep-Feo cells; Control, cells infected with AxshRNA-Control; HCV, cells treated with AxshRNA-HCV. In panels (b) and (c), cells were harvested on day 6 after adenovirus infection at an MOI of 1.

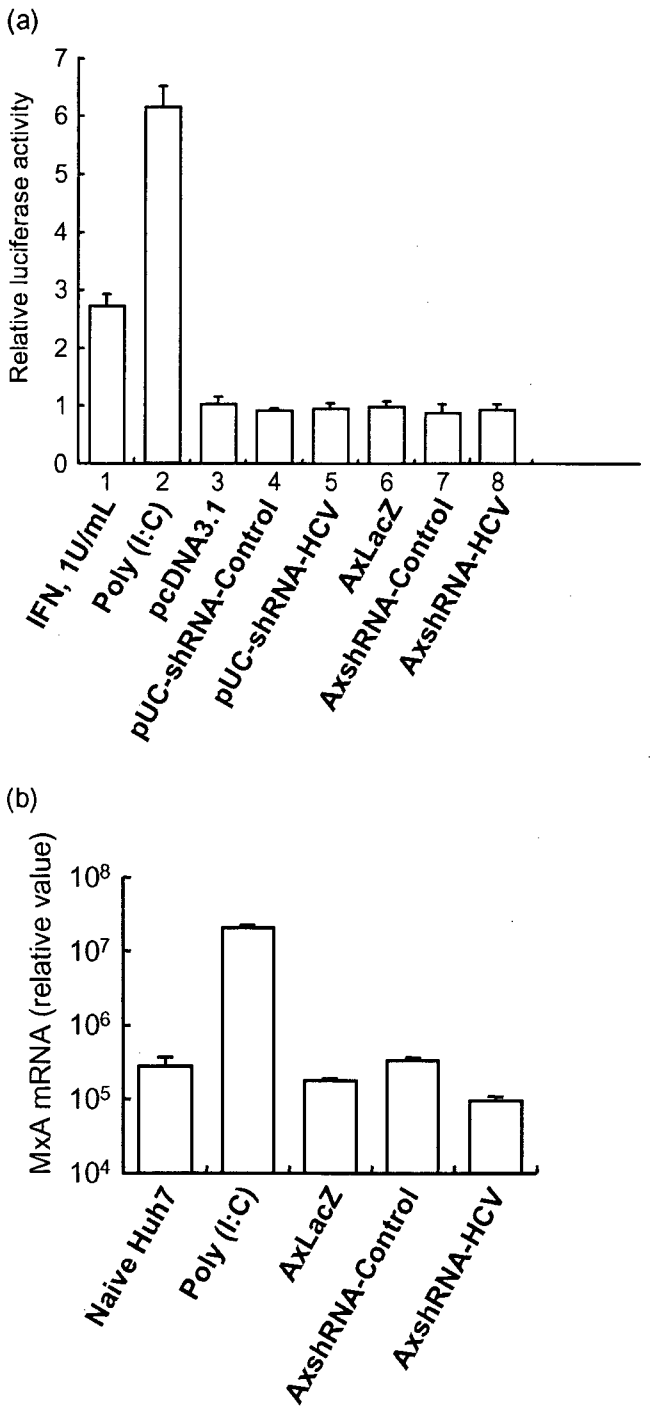

Figure 5 Interferon-stimulated gene responses by transfection of siRNA vectors. (a) Huh7 cells were seeded at 5×10^4 per well in 24-well plates on the day before transfection. As a positive control, 200 ng of pISRE-TA-Luc, or pTA-Luc, 1 ng of pRL-CMV, were transfected into a well using FuGENE-6 Transfection Reagent (Roche), and the cells were cultured with 1 U/mL of interferon (IFN) in the medium (lane 1). Lanes 3–5: 200 ng of pISRE-TA-Luc or pTA-Luc, and 1 ng of pRL-CMV were cotransfected with (lane2) 300 ng of poly (I : C), or 200 ng of plasmids (lane 3) pcDNA3.1, (lane 4) pUC19-shRNA-Control or (lane 5) pUC19-shRNA-HCV. Lanes 6–8: 200 ng of pISRE-TA-Luc or pTA-Luc, and 1 ng of pRL-CMV were transfected, and MOI = 1 of adenoviruses, (lane 6) AxLacZ, which expressed the beta-galactosidase (LacZ) gene under control of the chicken beta-actin (CAG) promoter as a control, (lane 7) AxshRNA-Control or (lane 8) AxshRNA-HCV were infected. Dual luciferase assays were performed at 48 h after transfection. The Fluc activity of each sample was normalized by the respective Rluc activity, and the respective pTA luciferase activity was subtracted from the pISRE luciferase activity. The experiment was done in triplicate, and the data are displayed as means + SD. (b) Huh7 cells were infected with indicated recombinant adenoviruses, AxLacZ, AxshRNA-Control and AxshRNA-HCV. RNA was extracted from each sample at day 6, and mRNA expression levels of an interferon-inducible MxA protein were quantified by the real-time RT-PCR analysis. Primers used were as follows: human MxA sense, 5′-CGA GGG AGA CAG GAC CAT CG-3′; human MxA antisense, 5′-TCT ATC AGG AAG AAC ATT TT-3′; human beta-actin sense, 5′-ACA ATG AAG ATC AAG ATC ATT GCT CCT CCT-3′; and human beta-actin antisense, 5′-TTT GCG GTG GAC GAT GGA GGG GCC GGA CTC-3′.

negative- or positive-control shRNA plasmids was transfected. (Fig. 5a). Similarly, the expression levels of an interferon-inducible MxA protein did not significantly change by transfection of shRNA-expression vectors (Fig. 5b). These results demonstrate that the shRNA used in the present study lack induction of the ISG responses both in the form of the expression plasmids and the adenovirus vectors.

Effect of siRNA and shRNA adenoviruses on HCV-JFH1 cell culture

The effects of HCV-targeted siRNA- and shRNA-expressing adenoviruses were confirmed by using HCV-JFH1 virus cell culture system. Transfection of the siRNA #331[14] into HCV-infected Huh7.5.1 cells resulted in substantial decrease of intracellular HCV RNA, while a control siRNA showed no effect (Fig. 6a). Similarly, infection of AxshRNA-HCV into Huh7.5.1/HCV-JFH1 cells specifically suppressed expression of HCV RNA (Fig. 6b).